第 33 卷第 11 期 无 机 化 学 学 报 Vol.33 No.11
2017 年 11 月 CHINESE JOURNAL OF INORGANIC CHEMISTRY 2031-2037

一个具有 *eea* 拓扑和高甲烷存储量的金属有机骨架材料

季卿妍[1] 王 倩*,[1] 李洪昕[1] 薛东旭[1] 白俊峰*,[1,2]
([1]陕西师范大学化学化工学院,应用表面与胶体化学教育部重点实验室,西安 710062)
([2]南京大学化学化工学院,配位化学国家重点实验室,南京 210093)

摘要:合成了含有 2 个羧基和 1 个 N 配位点的双官能团有机配体 5-(quinolin-6-yl)isophthalic acid (H_2L),并成功制得一个新的三维的多孔金属-有机骨架{[CuL]·x(Solvent)}$_n$ (**1**)。金属–有机骨架 **1** 具有 *eea* 拓扑的网络结构,点(Schläfli)符号为{$4^2.6$}$_2${$4^4.6^2.8^6.10^3$}。值得一提的是,除去溶剂分子的 **1** 还表现出较大的 CH_4 吸附焓,在 298 K 和高压下对 CH_4 有高的吸附量。

关键词:Cu(Ⅱ)配合物;*eea* 拓扑的网络结构;CH_4 吸附
中文分类号:O614.121 **文献标识码**:A **文章编号**:1001-4861(2017)11-2031-07
DOI:10.11862/CJIC.2017.245

An eea Topological Metal-Organic Framework with High Methane Uptake

JI Qing-Yan[1] WANG Qian*,[1] LI Hong-Xin[1] XUE Dong-Xu[1] BAI Jun-Feng*,[1,2]
([1]*Key Laboratory of Applied Surface and Colloid Chemistry, Ministry of Education, School of Chemistry & Chemical Engineering, Shaanxi Normal University, Xi'an* 710062, *China*)
([2]*State Key Laboratory of Coordination Chemistry, School of Chemistry and Chemical Engineering, Nanjing University, Nanjing* 210093, *China*)

Abstract: A new 3D porous MOF, {[CuL]·x(Solvent)}$_n$ (**1**) have been successfully synthesized based upon a bifunctional organic ligand with two carboxyl groups and one nitrogen donor of 5-(quinolin-6-yl)isophthalic acid (H_2L). MOF **1** exhibits an *eea* topological network with the point (Schläfli) symbol of {$4^2.6$}$_2${$4^4.6^2.8^6.10^3$}. Remarkably, desolvated **1** performs a high CH_4 adsorption enthalpy and high methane uptake at high pressure and 298 K. CCDC: 1559215, desolvated **1**.

Keywords: Cu(Ⅱ) complex; eea topology; CH_4 storage

Storage of natural gas (NG), comprising mainly methane, has attracted wide attention due to the concerns over national and regional energy security, ground-level air quality, and climate change[1-2]. Considering its naturally abundant and relatively environmentally friendly compared to conventional liquid hydrocarbon fuels, methane has been regarded as one of the most attractive and promising alternative source of clean energy[3-5]. However, owing to its low volumetric energy density at standard conditions, the efficient storage of methane in a limited volume has become a major challenge for its on-board applications[4,6]. Compared with the compressed natural gas (CNG) realized at high pressure and liquefied natural gas (LNG) stored at low temperature, adsorptive natural gas (ANG) is a possible and effective approach, in which the high storage of methane can be achieved near room temperature and at moderate pressures through

收稿日期:2017-07-21。收修改稿日期:2017-09-13。
长江学者计划和陕西省百人计划资助项目(No.)资助项目。
*通信联系人。E-mail:wangq@snnu.edu.cn,bjunfeng@nju.edu.cn,Tel:025-89683384

efficient packing of the fluid molecules in nanospaces of the porous materials[5,7-9].

Different from the low surface area of zeolites and the difficulties in tuning of structures for activated carbons[10-11], metal-organic frameworks (MOFs), which have emerged as an intriguing class of porous material, combine with the advantages of ultra-high surface, versatile and designable structures, high pore volume and tunable pores, et al.[12-18]. Thus, this kind of material which displays the great potential applications in the gas storage would be developed to discover more fascinating methane storage properties. Moreover, the MOF materials available to the real-word CH_4 on-board applications are still rare. Hence, further exploring MOFs with good CH_4 storage properties is still a great task and challenge for synthetic chemists.

We are of great interest in the design and construction of 3D porous functional MOFs from both symmetric and unsymmetric multidentate organic ligands with promising gas adsorptions, i.e., CH_4 storage[19-30]. Recently, bifunctional organic ligands with two carboxyl groups and one nitrogen donor have been largely used to construct MOFs for the investigations of their CO_2 capture properties[23,25-26,29]. However, for the study of methane storage, MOFs based on this type of ligands are still rarely developed[28]. Thus, in this paper, we utilized a bifunctional organic ligand of 5-(quinolin-6-yl)isophthalic acid (H_2L) and dicopper-paddlewheel units to assemble a new 3D porous MOF, $\{[CuL]\cdot x(Solvent)\}_n$ (**1**). In this work, we achieved an *eea* topological MOF with the point (Schläfli) symbol of $\{4^2.6\}_2$ $\{4^4.6^2.8^6.10^3\}$. Remarkably, desolvated **1** exhibits a high CH_4 adsorption enthalpy and high methane uptake amount at high pressure and 298 K.

1 Experimental

1.1 Materials and methods

All reagents were obtained from commercial vendors and, unless otherwise noted, were used without further purification ($CuCl_2\cdot 2H_2O$, Sinopharm Chemical Reagent, AR, 99%; 6-bromoquinoline, TCI, GC, 95%; 3,5-bis (methoxy-carbonyl)phenylboronic acid, Ark, ≥95%). The FT-IR spectra were obtained in the 4 000~400 cm^{-1} on a VECTOR TM 22 spectrometer using KBr pellets. ^1H NMR spectra were recorded on a Bruker DRX-300 spectrometer with tetramethylsilane as an internal reference. Thermal gravimetric analyses (TGA) were performed under N_2 atmosphere (100 $mL\cdot min^{-1}$) with a heating rate of 5 ℃ $\cdot min^{-1}$ using a 2960 SDT thermogravimetric analyzer. Powder X-ray diffraction (PXRD) data were collected over the 2θ range 5°~50° on a Bruker D8 ADVANCE X-ray diffractometer using Cu $K\alpha$ radiation (λ=0.154 18 nm) at 40 kV and 40 mA.

1.2 Synthesis of 5-(quinolin-6-yl)isophthalic acid (H_2L)

To a solution of 6-bromoquinoline (2.1 g, 10 mmol) in 125 mL of toluene was added the mixture of 3,5-bis (methoxy-carbonyl)phenylboronic acid (3.2 g, 12 mmol) in 30 mL of ethanol, followed by the addition of a solution of Na_2CO_3 (3.5 g, 33 mmol) in 10 mL of water. This solution was degassed using N_2 for 10 min, and then $Pd(PPh_3)_4$ (0.5 g, 0.43 mmol) was added. The resulting reaction mixture was stirred at 90 ℃ under N_2 overnight. The solvent was then removed using rotary evaporation, and the residue was dissolved in CH_2Cl_2 and washed with water. The organic layer was subsequently dried over $MgSO_4$, filtered, concentrated, and purified by silica gel flash column chromatography with an eluent of acetone/petroleum ether (1:10, *V*/*V*). The product was hydrolyzed by refluxing in 2 $mol\cdot L^{-1}$ aqueous KOH followed by acidification with 37%(*w*/*w*) HCl to afford a white solid of H_2L. Yield: 1.7 g (58%). FT-IR (KBr, cm^{-1}): 1 720, 1 595, 1 406, 1 226, 1 068, 923, 896, 827, 802, 769, 705, 678, 474. ^1H NMR (DMSO-d_6): δ 13.51 (broad peak, COOH), 9.07 (d, 1H, ArH), 8.76 (d, 1H, ArH), 8.58 (s, 3H, ArH), 8.53 (s, 1H, ArH), 8.32 (d, 1H, ArH), 8.24 (d, 1H, ArH), 7.79 (m, 1H, ArH).

1.3 Synthesis of $\{[CuL]\cdot x(Solvent)\}_n$ (1)

A solution of $CuCl_2\cdot 2H_2O$ (25.0 mg, 0.147 mmol) in 0.5 mL of methanol was mixed with the H_2L (10 mg, 0.034 mmol) in 1.5 mL of *N*,*N*-dimethylformamide. To this was added 0.08 mL of concentrated HNO_3 with stirring. The mixture was sealed in a Pyrex tube and

heated to 100 ℃ for 48 h. The green block crystals obtained were filtered and washed with DMF. Yield: 85%. Selected IR (cm^{-1}): 1 646, 1 585, 1 507, 1 448, 1 380, 1 089, 839, 779, 730, 487.

1.4 Crystal structure determination

Single-crystal X-ray diffraction data were measured on a Bruker Apex Ⅱ CCD diffractometer at 150(2) K using graphite monochromated Mo $K\alpha$ radiation (λ=0.071 073 nm). Data reduction was made with the Bruker SAINT program. The structures were solved by direct methods and refined with full-matrix least squares technique using the SHELXTL package[31]. Non-hydrogen atoms were refined with anisotropic displacement parameters during the final cycles. Organic hydrogen atoms were placed in calculated positions with isotropic displacement parameters set to $1.2U_{eq}$ of the attached atom. The unit cell includes a large region of disordered solvent molecules, which could not be modelled as discrete atomic sites. We employed PLATON/SQUEEZE[32] to calculate the diffraction contribution of the solvent molecules and, thereby, to produce a set of solvent-free diffraction intensities; structures were then refined again using the data generated. Crystal data and refinement conditions are shown in Table 1.

CCDC: 1559215, desolvated **1**.

Table 1　Crystal data and structure refinement for desolvated compound 1

Empirical formula	$C_{17}H_9CuNO_4$	Crystal size / mm	0.210×0.130×0.080
Formula weight	354.79	θ range for data collection / (°)	1.764~28.306
Crystal system	Trigonal	Index ranges	$-24 \leqslant h \leqslant 20, -24 \leqslant k \leqslant 24, -92 \leqslant l \leqslant 92$
Space group	$R\bar{3}c$	Reflection collected	48 147
a / nm	1.867 89(8)	Independent reflection	5 770 (R_{int}=0.153 5)
b /nm	1.867 89(8)	Completeness to θ=20.879° / %	99.70
c / nm	6.925 9(11)	Refinement method	Full-matrix least-squares on F^2
Volume / nm^3	20.927(4)	Data, restraint, parameter	5 770, 0, 208
Z	36	Goodness-of-fit on F^2	0.983
D_c / ($Mg\cdot m^{-3}$)	1.013	Final R indices [$I>2\sigma(I)$]	R_1=0.045 0, wR_2=0.104 5
Absorption coefficient / mm^{-1}	0.951	R indices (all data)	R_1=0.109 0, wR_2=0.134 1
F(000)	6 444	Largest diff. peak and hole / ($e\cdot nm^{-3}$)	521 and −448

1.5 Gas sorption measurements

Low-pressure sorption isotherms of CH_4 (99.999%) and N_2 (99.999%) gas were performed on Quantachrome Autosorb IQ-2 surface area and pore size analyzer. High pressure excess adsorptions of CH_4 gas (99.999%) were measured using a Rubotherm ISOSORP-HyGpra+V adsorption instrument over a pressure range of 0~10 MPa at 298 K. Before analysis, the as-synthesized samples of **1** were soaked in acetone for 3 days with acetone refreshing every 8 hours. Then, the acetone-exchanged sample was activated at 80 ℃ and under vacuum for 10 hours.

2 Results and discussion

2.1 Crystal structure of compound 1

Solvothermal reaction of $CuCl_2\cdot 2H_2O$ with H_2L in the solution of DMF/MeOH containing HNO_3 afforded a high yield of green block crystals of compound **1**. The single X-ray crystal diffraction reveals that **1** crystallizes in trigonal space group $R\bar{3}c$. In **1**, the dicopper-paddlewheel units are interconnected by the L^{2-} organic ligand, leading to the formation of a 3D porous framework (Fig.1). The structure consists of two types of cages: trigonal antiprism (cage A) and cuboctahedron (cage B), in which, the cage A is comprised by six Cu-paddlewheel units and six L^{2-} with each side of the trigonal antiprism occupied by one organic ligand, and the cage B is consisted of twelve dicopper-paddlewheel units and six L^{2-} with each triangular side of the cuboctahedron occupied by one organic ligand and leaving its rectangular sides serving as the windows of cage B, respectively (Fig. 1b). Then, each cage A is surrounded by eight cages B through face-sharing, and simultaneously, each cage

B is extended through eight cages A by sharing their triangular faces, too, which leads to the formation of the three-dimensional porous framework of compound **1** (Fig.1c,d). Determined by the van der Waals diameter of the inserted pseudo atom, the pore size of cage A and cage B is 0.74 and 0.9 nm, respectively. The total potential solvent accessible volumes in desolvated compound **1** calculated by the PLATON/SOLV program is *ca.* 49.6% and its framework density is 1.013 $g \cdot cm^{-3}$.

To better understand the structure, the dicopper-

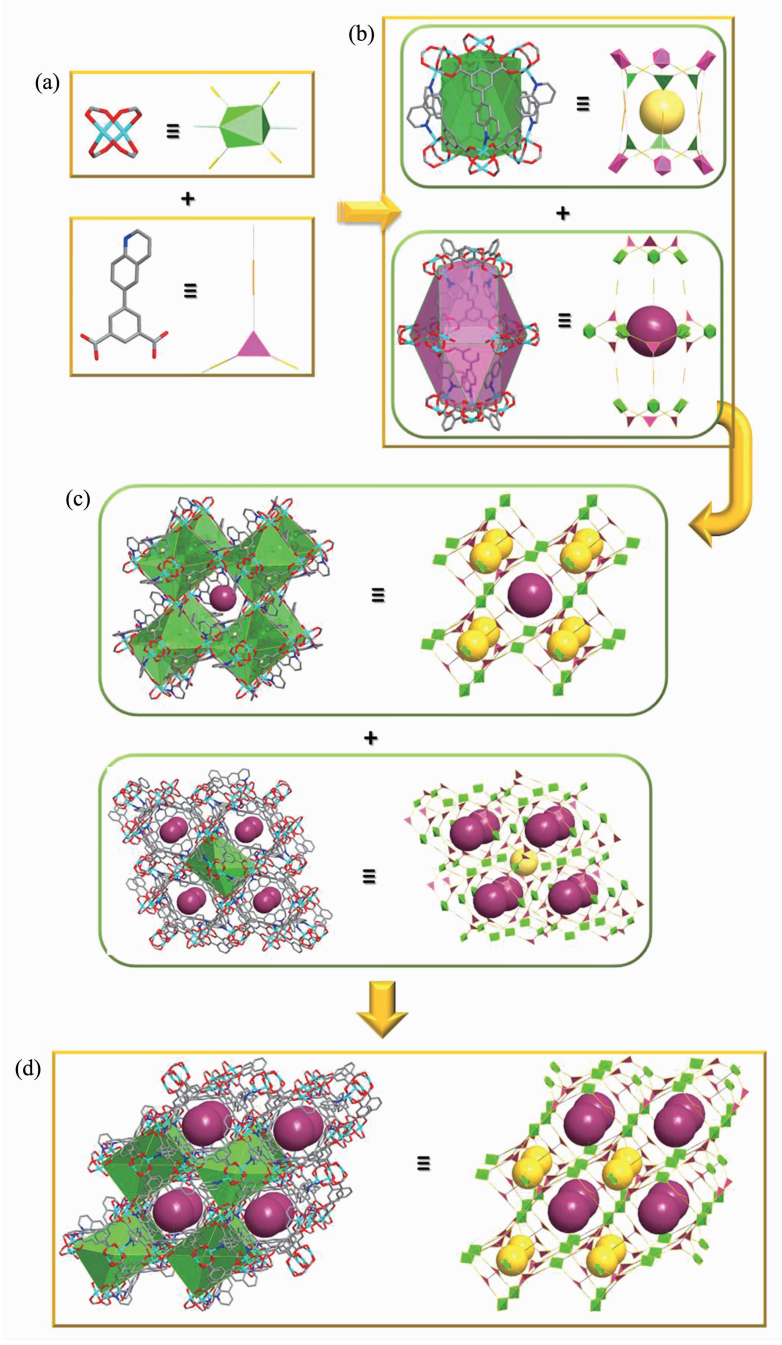

Hydrogen atoms are omitted for clarity; Cu: turquiose, C: gray, N: blue, O: red

Fig.1 (a) Inorganic (left) and organic (right) secondary building units (SBUs) in compound **1**; (b) Trigonal antiprism (cage A, up) and cuboctahedron (cage B, bottom) in compound **1**; (c) One cage A surrounded by eight cages B through face-sharing (up) and one cage B surrounded by eight cages A through face-sharing (bottom); (d) 3D porous framework (left) of compound **1** and its topological network (right)

paddlewheel unit is simplified as 6-connected node, and the organic ligand serve as a 3-connected node, then **1** may be described as a (3,6)-connected *eea*-topological network with its point (Schläfli) symbol of $\{4^2.6\}_2\{4^4.6^2.8^6.10^3\}$ (Fig.1).

2.2 Thermal stabilities and powder X-ray diffraction

The thermogravimetric analysis (TGA) of as-synthesized compound **1** was performed to confirm its thermal stability. As shown in Fig.2, **1** exhibits an obvious weight-loss process. The first stage is observed before 220 ℃, which corresponds to the removal of solvent molecules in the pores. The second one is around 320 ℃, which should be ascribed to the decomposition of the organic ligand and the collapse of the dicopper-paddlewheel unit.

The powder X-ray diffraction (PXRD) has been measured to confirm the phase purity of the bulk sample (Fig.3). The patterns of the as-synthesized sample are well coincident with the simulated one derived from the X-ray single crystal data, implying the phase purity of the bulk sample. In addition, the PXRD patterns of activated compound **1** that is coincident with the as-synthesized one also indicate the integrality of its framework after the removal of solvent molecules.

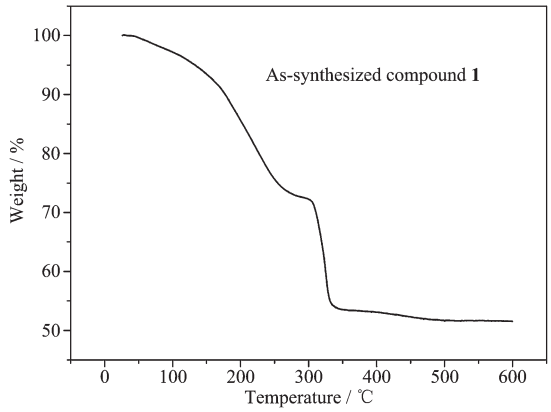

Fig.2　TGA curve of the as-synthesized **1**

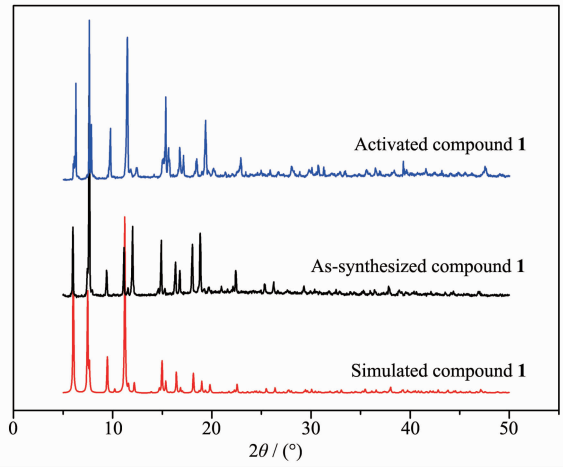

Fig.3　PXRD patterns of the simulated, as-synthesized and activated **1**

2.3 Surface area and porosity

To evaluate the permanent porosity of desolvated compound **1**, its N_2 sorption isotherm at 77 K was measured. As a result, the N_2 uptake is 330 $cm^3 \cdot g^{-1}$ (STP) at 100 kPa (Fig.4). The N_2 gas sorption shows a reversible type Ⅰ isotherm without hysteresis on desorption, which is characteristic of microporous material. The Brunaer-Emmett-Teller (BET) and Langmuir surface area of desolvated compound **1** were estimated to be 1 177 and 1 337 $m^2 \cdot g^{-1}$, respectively. Furthermore, its NLDFT (nonlocal density functional theory) pore diameters are 0.6 and 0.8 nm, which is in great agreement with the pore size as determined from the crystal structure. Based on N_2 adsorption uptake at P/P_0 =0.974, the total pore volume of desolvated **1** was estimated to be 0.5 $cm^3 \cdot g^{-1}$.

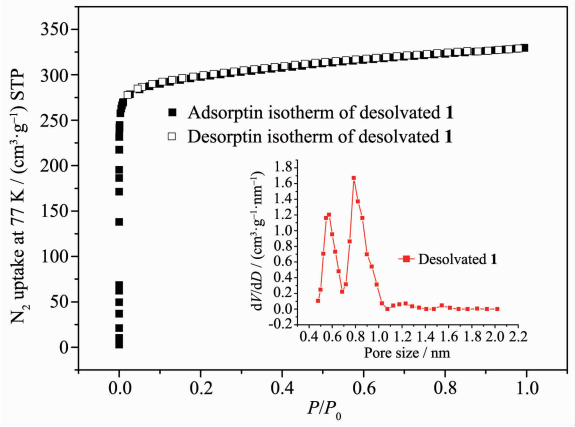

Inset: pore size distribution curve of desolvated **1**

Fig.4　N_2 adsorption-desorption isotherms for desolvated compound **1** at 77 K

2.4 Low pressure methane sorption

The high surface area of desolvated **1** prompted us to further investigate its methane adsorption property. The CH_4 low-pressure (0~100 kPa) sorption isotherms of activated **1** were measured at 273 and 298 K (Fig.

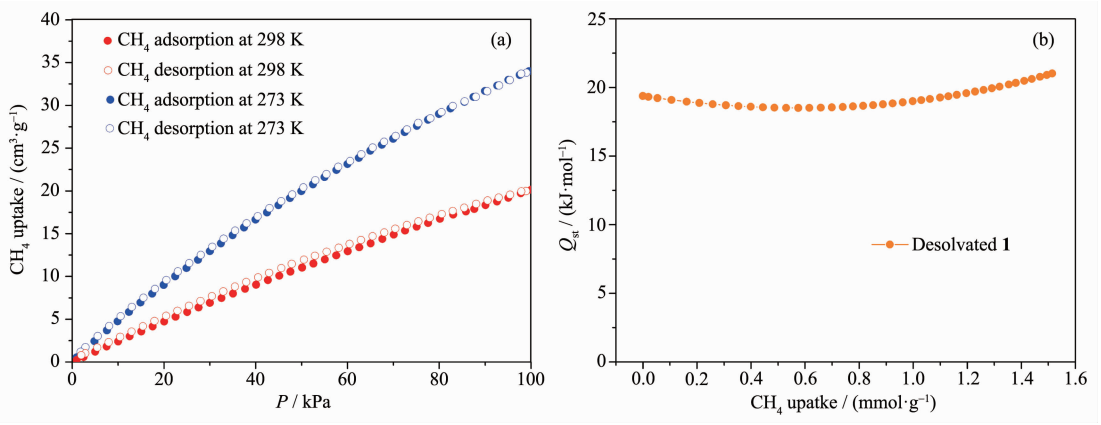

Fig.5 (a) CH_4 adsorption-desorption isotherms for desolvated compound **1**; (b) CH_4 adsorption enthalpy of desolvated **1**

5a), respectively. At 100 kPa, desolvated compound **1** takes up CH_4 with the amount of 34 and 20 $cm^3 \cdot g^{-1}$ at 273 and 298 K, respectively. Based upon the experimental isotherm data at 273 and 298 K (Fig.5b), the isosteric heat (Q_{st}) of CH_4 adsorption was calculated to be 19.4 $kJ \cdot mol^{-1}$ at zero loading by the virial method, indicating a relatively strong interaction between its frameworks and the adsorbed CH_4 molecules. This value is close to the corresponding values found for most promising MOFs for methane storage[10].

2.5 High pressure methane adsorption

To further evaluate the methane storage capability of desolvated **1**, its high-pressure CH_4 sorption isotherms were also measured in the pressure range of 0~10 MPa at 298 K. As shown in Fig.6, at 3 500 kPa, the moderately practical condition for CH_4 storage, desolvated compound **1** shows a total gravimetric uptake of 137 $cm^3 \cdot g^{-1}$ (STP). Moreover, at 6 500 and 10 000 kPa, the total methane uptake amounts of desolvated **1** are further increased to 162 and 185 $cm^3 \cdot g^{-1}$ (STP), respectively. More interestingly, when the crystal density is considered, the total volumetric methane total uptakes of activated compound **1** are 138, 164 and 187 cm_{gas}^3 (STP)$\cdot cm_{ads}^{-3}$ at 3 500, 6 500 and 10 000 kPa, respectively. These values are among the relatively high range of the reported porous MOFs, which indicates this MOF might serve as a good potential candidate for methane storage application[8].

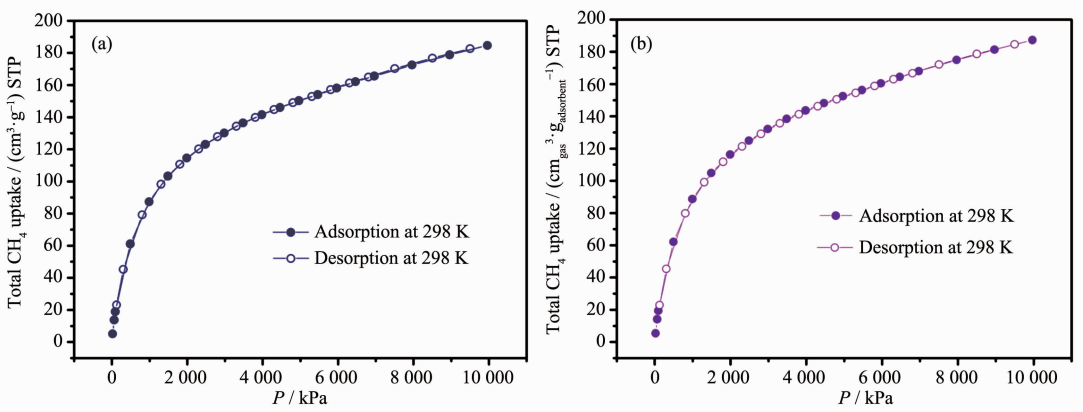

Fig.6 Total CH_4 gravimetric (a) and volumetric (b) uptake of desolvated **1** at 298 K

3 Conclusions

In conclusion, based upon an organic ligand of 5-(quinolin-6-yl)isophthalic acid, a new 3D porous MOF **1**, has been successfully constructed with a rare (3,6)-connected eea topological network, of which the point (Schläfli) symbol is $\{4^2.6\}_2$ $\{4^4.6^2.8^6.10^3\}$. More interestingly, this activated MOF performs a large CH_4 adsorption enthalpy and high methane uptake amount at high pressure and 298 K.

References:

[1] Peng Y, Krungleviciute V, Eryazici I, et al. *J. Am. Chem. Soc.*, **2013**,**135**:11887-11894

[2] Wu H, Simmons J M, Liu Y, et al. *Chem. Eur. J.*, **2010**,**16**:5205-5214

[3] He Y B, Zhou W, Qian G D, et al. *Chem. Soc. Rev.*, **2014**, **43**:5657-5678

[4] He Y B, Zhou W, Yildirim T, et al. *Energy Environ. Sci.*, **2013**,**6**:2735-2744

[5] Kowalczyk P, Solarz L, Do D D, et al. *Langmuir*, **2006**,**22**:9035-9040

[6] Mendoza-Cortés J L, Han S S, Furukawa H, et al. *J. Phys. Chem. A*, **2010**,**114**:10824-10833

[7] Wilmer C E, Farha O K, Yildirim T, et al. *Energy Environ. Sci.*, **2013**,**6**:1158-1163

[8] Mason J A, Veenstra M, Long J R. *Chem. Sci.*, **2014**,**5**:32-51

[9] Li B, Wen H M, Wang H L, et al. *J. Am. Chem. Soc.*, **2014**, **136**:6207-6210

[10]Makal T A, Li J R, Lu W G, et al. *Chem. Soc. Rev.*, **2012**, **41**:7761-7779

[11]Li J R, Kuppler R J, Zhou H C. *Chem. Soc. Rev.*, **2009**,**38**:1477-1504

[12]Klein N, Senkovska I, Gedrich K, et al. *Angew. Chem. Int. Ed.*, **2009**,**48**:9954-9957

[13]Gedrich K, Senkovska I, Klein N, et al. *Angew. Chem. Int. Ed.*, **2010**,**49**:8489-8492

[14]Ma S Q, Zhou H C. *Chem. Commun.*, **2010**,**46**:44-53

[15]Tan Y X, He Y P, Zhang J. *Chem. Commun.*, **2011**,**47**:10647-10649

[16]Perry J J, Perman J A, Zaworotko M J. *Chem. Soc. Rev.*, **2009**,**38**:1400-1417

[17]Yang E C, Ding B, Liu Z Y, et al. *Cryst. Growth Des.*, **2012**,**12**:11851192

[18]Zhuang W, Yuan D, Liu D, et al. *Chem. Mater.*, **2012**,**24**:18-25

[19]Yun R R, Lu Z Y, Pan Y, et al. *Angew. Chem.*, **2013**,**125**:11492-11495

[20]Duan J G, Yang Z, Bai J F, et al. *Chem. Commun.*, **2012**, **48**:3058-3060

[21]Zheng B S, Yang Z, Bai J F, et al. *Chem. Commun.*, **2012**, **48**:7025-7027

[22]Zhang M X, Li B, Li Y Z, et al. *Chem. Commun.*, **2016**,**52**:7241-7244

[23]Yun R R, Duan J G, Bai J F, et al. *Cryst. Growth Des.*, **2013**,**13**:24-26

[24]Zheng B S, Bai J F, Duan J G, et al. *J. Am. Chem. Soc.*, **2011**,**133**:748-751

[25]Du L T, Lu Z Y, Zheng K Y, et al. *J. Am. Chem. Soc.*, **2013**,**135**:562-565

[26]Jiang J J, Wang Q, Zhang M X, et al. *Cryst. Growth Des.*, **2017**,**17**:2223-2227

[27]Lu Z Y, Bai J F, Hang C, et al. *Chem. Eur. J.*, **2016**,**22**:6277-6285

[28]Wang Q, Song X H, Zhang M X, et al. *Cryst. Growth Des.*, **2016**,**16**:6156-6159

[29]Wang Q, Jiang J J, Zhang M X, et al. *Cryst. Growth Des.*, **2017**,**17**:16-18

[30]Lu Z Y, Du L T, Tang K Z, et al. *Cryst. Growth Des.*, **2013**, **13**:2252-2255

[31]Sheldrick G M. *Acta Crystallogr., Sect. A*: *Found. Crystallogr.*, **2008**,**A64**:112-122

[32]Spek A L. *J. Appl. Crystallogr.*, **2003**,**36**:7-13